NJC

PAPER

Check for updates

From CO$_2$ to CS$_2$: a theoretical investigation of the cycloaddition to aziridines mediated by metal-free porphyrin-based catalytic systems†

Caterina Damiano, [ID] *[a] Nicola Panza, [ID] [a] Jakub Nagy,[b] Emma Gallo [ID] [a] and Gabriele Manca [ID] *[c]

A detailed computational analysis of the synthesis of thiazolidine-2-thiones by CS$_2$ insertion into three membered aziridine rings is here reported. DFT studies highlighted the feasibility of the atom-efficient process by employing either the metal-free binary TPPH$_2$/TBACl system or bifunctional TPPH$_4$Cl$_2$ molecules as the catalytic species. Detailed investigations into the mechanism promoted by the TPPH$_2$/TBACl system indicated, as in the analogous cycloaddition of CO$_2$, the pivotal role of the adduct between TPPH$_2$ and TBACl salts in the synthesis of both *N*-aryl and *N*-alkyl thiazolidine-2-thiones. The latter species can be also obtained by using the eco-compatible TPPH$_4$Cl$_2$ catalyst, which is able to simultaneously activate CS$_2$ and aziridine molecules. The comparison of the overall energy gains of the reaction between aziridines and CS$_2$ with respect to the same process involving CO$_2$ revealed that the formation of thiazolidine-2-thiones is more favoured than the synthesis of oxazolidin-2-ones paving the way to develop efficient and eco-compatible synthesis of thiazolidine-2-thiones.

Introduction

The synthesis of medium size N-heterocycles is one of the most dynamic and constantly evolving areas of chemistry in view of the widespread occurrence of N-heterocyclic fragments in various biologically and pharmaceutically active molecules. Among all the naturally and synthetically derived N-heterocycles, increasing interest has been devoted to the sulphur containing ones, which have proved to be very promising bioactive spiecies[1] and chiral auxiliaries in organic synthesis.[2] In particular, the five-membered thiazolidine-2-thione scaffold has aroused great attention due to its activity as a regulator of cancer cells apoptosis,[3] inhibitor of the aldose reductase and xanthine oxidase[4] and anti-inflammatory and antifungal agents.[5]

Considering the potential applicability of thiazolidine-2-thiones, many efforts have been devoted to developing synthetic methodologies that are more efficient and sustainable than the conventional ones. Traditionally, thiazolidine-2-thiones, which are the sulphur analogous of oxazolidin-2-ones, can be synthesised by

reacting amino alcohols with high concentration of carbon disulphide (CS$_2$) under harsh reaction conditions (high temperatures, strong alkaline solutions, and extended reaction times).[6] In order to overcome these experimental drawbacks and increase the process sustainability, microwave-assisted syntheses[7] and various multicomponent reactions have been developed. The latter include: (i) the iodocyclization of allyl amines, carbon disulphide and iodine;[8] (ii) the three-component coupling of amines, alkynes and aldehydes followed by the cyclization with CS$_2$;[9] (iii) the three-component one-pot reaction of amines, CS$_2$ and either α-bromoketones[10] or α-chloro-β,γ-alkenoate esters[11] and (iv) the phosphine-catalysed one-pot reaction between dithiocarbamates (prepared *in situ* from amines and CS$_2$) and arylpropiolates.[12] However, one of the most attractive procedures in terms of atom-economy is the CS$_2$ cycloaddition to aziridine rings. It is important to note that this approach allows the combination of a 100% atom-efficient process with an alternative disposal of carbon disulphide. In fact, CS$_2$ plays a central role in many industrial sectors, such as chemical fiber plants (*e.g.* viscose production) or petroleum processing, but it is particularly harmful[13] and its common disposal requires an incineration with the consequent emission in the atmosphere of pollutant gases (*e.g.* CO$_2$, SO$_2$ or H$_2$S) with many environmental negative effects.[14]

Even if the CS$_2$ cycloaddition to aziridines offers several advantages and shows analogous characteristics to the synthesis of oxazolidin-2-ones from aziridines and CO$_2$, it has been much less studied both from the experimental and theoretical

[a] Department of Chemistry, University of Milan, Via Golgi 19, I-20133, Milan, Italy. E-mail: caterina.damiano@unimi.it
[b] Faculty of Science in Department of Chemistry, Masaryk University, Czech Republic
[c] Istituto di Chimica dei Composti OrganoMetallici, CNR-ICCOM, Via Madonna del Piano 10, I-50019, Sesto Fiorentino, Italy. E-mail: gabriele.manca@iccom.cnr.it
† Electronic supplementary information (ESI) available. See DOI: https://doi.org/10.1039/d2nj05479e

point of view. To date, only a few examples of organo- and metal-based catalytic systems capable of promoting this reaction have been reported in the literature and they usually require high catalytic loadings of alkali metal halides,[15] tributylphosphine,[16] pyrrolidine,[17] pyridinecarboxaldehyde oxime,[18] amidato divalent lanthanide complexes[19] or MOFs based on the trivalent dysprosium center.[20]

Considering the analogy between CO_2 and CS_2, it is reasonable to think that catalytic systems, optimised for the synthesis of oxazolidin-2-ones, could be equally efficient in the synthesis of thiazolidine-2-thiones from aziridines and CS_2.

In the recent years we have investigated the catalytic activity of porphyrin-based systems in the CO_2 cycloaddition to aziridines[21–24] and the symbiotic computational/experimental approach has highlighted the high efficiency of the metal-free TPPH$_2$/TBACl binary catalyst (TPP = dianion of tetraphenyl porphyrin, TBACl = tetrabutyl ammonium chloride) in promoting the synthesis of *N*-alkyl and *N*-aryl oxazolidine-2-ones under both homogenous and heterogeneous conditions.[25] DFT calculations pointed out the formation of the active adduct **1** (Scheme 1) where the butyl substituents of the TBA$^+$ cation are perfectly hosted in the crib formed by the peripheral *meso* substituents of the porphyrin macrocycle. Adduct **1** has been estimated to be more stable by *ca.* -7.5 kcal mol^{-1} in free energy than the separated components due to the cooperative effects of the dispersion and weak forces between the alkyl chains of TBA$^+$ and the aromatic framework of TPPH$_2$. Adduct **1** is the real catalyst of the process by weakening the ionic interactions between TBA$^+$ and the chloride anion,

which makes the latter more prone to attack the aziridine ring with the following formation of intermediate **3**.

At this point, the former aziridine nitrogen atom has acquired a sufficient basic character to activate carbon dioxide with the consequent synthesis of *N*-alkyl and *N*-aryl oxazolidin-2-ones.

The nature of the R substituents (alkyl or aryl) does not affect the reaction mechanism and only small variations in the height of the barriers or in the energy stabilization of the encountered intermediates were observed.

It is worth noting that additional experimental studies revealed the possibility of replacing the binary TPPH$_2$/TBACl system with the more convenient bifunctional TPPH$_4$Cl$_2$ catalyst to promote CO_2 cycloaddition (Scheme 1).[26] The very cheap and eco-compatible latter catalyst, simply obtained by treating TPPH$_2$ with HCl, efficiently mediated the synthesis of *N*-alkyl oxazolidin-2-ones in the absence of any Lewis acid or additive. DFT studies of the reaction mechanism revealed that the TPPH$_4$Cl$_2$ catalyst allows the synthesis of *N*-alkyl oxazolidin-2-ones through the simultaneous activation of aziridine and CO_2 molecules by forming an adduct between all the three species involved in the reaction (TPPH$_4$Cl$_2$, aziridine and CO_2). This synergic activation can occur thanks to the co-presence of the porphyrin skeleton and the nucleophilic chloride anion, which are responsible for the reaction regioselectivity and the ring-opening of the aziridine moiety, respectively.

The intriguing results that were obtained on CO_2 cycloadditions pushed us to investigate, from the computational point of view, the feasibility of the CS_2 cycloaddition to *N*-alkyl and *N*-aryl aziridines in the presence of either the binary TPPH$_2$/TBACl system or the bifunctional TPPH$_4$Cl$_2$ catalyst (Scheme 1) in order to pave the way for future experimental studies.
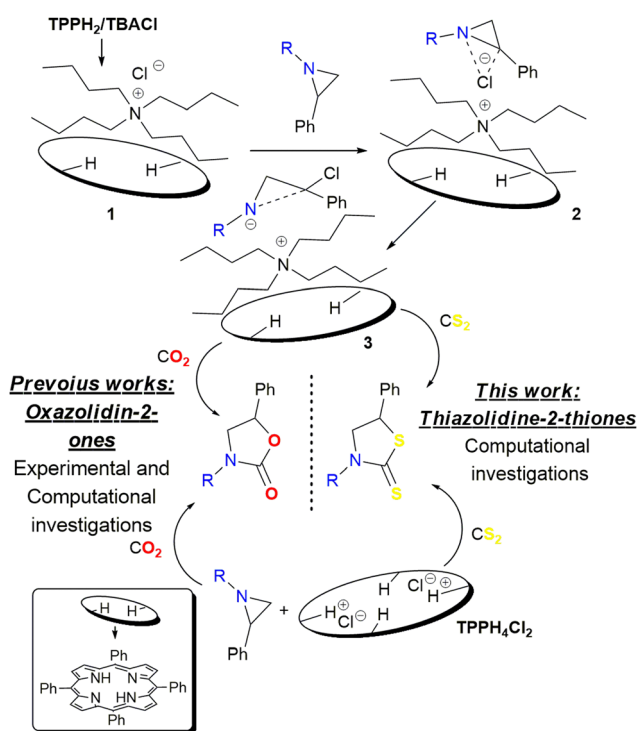
According to the reported studies of the CO_2 cycloaddition to aziridines, the catalytic activity of the binary TPPH$_2$/TBACl system was theoretically evaluated in the synthesis of both *N*-alkyl and *N*-aryl aziridines while the catalytic performance of the bifunctional TPPH$_4$Cl$_2$ catalyst was assessed in the sole CS_2 cycloaddition to *N*-alkyl aziridines.

Results and discussion

Binary TPPH$_2$/TBACl system for the CS_2 cycloaddition to aziridines

The precedent analysis of cycloaddition reactions involving CO_2 revealed that no productive reactions occurred between CO_2 and aziridine or TPPH$_2$ and that the first part of the mechanism is the formation of intermediate **3** (with R = alkyl or aryl substituent) that is responsible for the CO_2 activation. Thus, in order to confirm that this intermediate is the key-species also in the reaction between CS_2 and aziridines, preliminary studies were carried out on the reactivity of CS_2 towards either aziridine or TPPH$_2$.

The quasi null interaction between aziridine and CS_2, confirmed by the N$_{az}$–C(CS$_2$) distance longer than 3.2 Å, excluded any possible reaction between these two species in the early

Scheme 1 Catalytic activity of the TPPH$_2$/TBACl adduct (**1**) and the bifunctional TPPH$_4$Cl$_2$ catalyst in the reaction of aziridines with either CO_2 or CS_2.
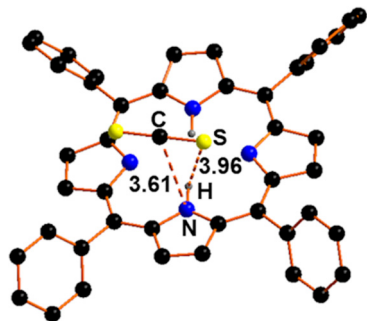
Fig. 1 Optimised structure of the hypothetical adduct between TPPH$_2$ and CS$_2$.

stage of the process. The formation of a possible adduct between porphyrin and the incoming CS$_2$ (Fig. 1) was also discharged for both structural (too long distance, 3.6 Å, between one N–H moiety and the carbon atom of CS$_2$) and disfavouring energy features (free energy cost of +3.4 kcal mol^{-1}). As shown in Fig. 1, CS$_2$ maintains the starting linear arrangement and any kind of perturbations are highlighted.

Once the possibility of a preliminary activation of CS$_2$ through an interaction with either aziridine or TPPH$_2$ macrocycle was discarded, we assumed that, as occurred in the case of CO$_2$, the catalytic cycle should evolve through the formation of the adduct **1** that interacts with the aziridine cycle forming the active species **3**. As pointed out in the previous articles on CO$_2$ activation, the encountered free energy barriers are high up to 40 kcal mol^{-1}, in agreement with the requested experimental conditions ($T > 80\ ^\circ$C). Two different typologies of N-substituted-2-phenylaziridines were modelled, which show on the nitrogen atom either the ^{n}butyl or the 3,5(CF$_3$)$_2$C$_6$H$_3$ aromatic substituent. The electrophilicity of the two aziridines was estimated by applying the procedure developed by Domingo et al.[27-30] In particular, the electrophilicity of N-aryl aziridine was estimated to be particularly greater than that of N-butyl one, with the electrophilicity index ω value of 2.28 vs. 1.3 eV that was calculated for N-butyl aziridine. This trend is in accordance with the higher free energy barrier (by ca. 10 kcal mol^{-1}) associated with the nucleophilic attack of chloride to N-butyl aziridine compared to that of Cl$^-$ to the aryl one. In both cases, the local electrophilicity index, ω_K^+, of the two aziridinic carbon atoms was estimated and it was found that the C$_1$ electrophilicity was double than that of C$_2$. In particular, while the ω_{C1}^+ and ω_{C2}^+ values of the N-aryl aziridine are 0.53 and 0.22, these values of N-butyl one are 0.31 and 0.14, respectively. These theoretical results are in agreement with the observed stereoselectivity as well as with the computed lower free energy barrier (ca. 8.5 kcal mol^{-1}) that was obtained for chloride attack to C$_1$ rather than to C$_2$ atom.

Considering that the formation of intermediate **3** is not affected by the nature of the other involved reagent (CO$_2$ or CS$_2$) the theoretical investigation of the formation of **3^{Bu}** (TPPH$_2$/TBACl + N-butyl-2-phenylaziridine) and **3^{Ar}** (TPPH$_2$/TBACl + N-aryl-2-phenylaziridine) has not been reported again but only indicated in the final free energy pathways of Fig. 4 and 6. All the calculations were performed by considering the tetrahydrofuran

(THF) as the reaction solvent, according to the experiments already performed for the CO$_2$ activation process.

CS$_2$ cycloaddition to N-alkyl aziridine. Computational investigations of the reactivity of CS$_2$ towards N-butyl-2-phenylaziridine were performed by analysing the electronic structure of the intermediate **3^{Bu}** species. The nucleophilicity of the nitrogen atom of the open species **3^{Bu}** was compared to that of the primary adduct **2^{Bu}** (Scheme 1). The obtained data revealed a nucleophilicity index of 1.8 eV and a local nucleophilic character (Nu$_{Naz}$) for the nitrogen atom of 0.9 eV. The nucleophilic character of N$_{az}$ in **3^{Bu}** was also certified by the plot of the HOMO-1 of **3^{Bu}** (Fig. S1, ESI†) showing the presence of an out-pointing lone pair at the N$_{az}$.

The direct interaction of the out-pointing lobe of N$_{az}$ with the carbon atom of CS$_2$, named C$_3$, is responsible for the desymmetrisation of carbon disulphide and the consequent formation of intermediate **4** (Fig. 2) with an energy gain of -17.1 kcal mol^{-1}.

It is important to note that the free energy gain estimated for the formation of **4** is comparable to that obtained for the CO$_2$ activation (estimated to be exergonic by -20.3 kcal mol^{-1}) and it suggests the suitability of the CS$_2$ cycloaddition to N-butyl-2-phenylaziridine. As reported in Fig. 3, intermediate **4** presents an already formed N$_{az}$–C$_3$ bond of 1.39 Å thanks to which the non-linear CS$_2$ moiety reaches a new SCS angle of 121°. The lack of linearity causes the appearance of an IR band at 552 cm^{-1} associated with the in phase C–S stretching, which is 100 cm^{-1} ca. red shifted with respect to the value computationally predicted for the free CS$_2$.

A Transition State, namely **4$_{TS}$** shown in Fig. 2 with a free energy barrier of +8.4 kcal mol^{-1} was isolated for the approaching of the CS$_2$ moiety to **3^{Bu}** species. The structure features the
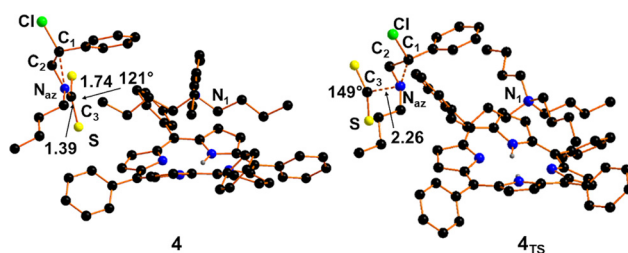

Fig. 2 Optimised structure of adduct **4** and the Transition State **4$_{TS}$**. Hydrogen atoms were omitted for clarity.
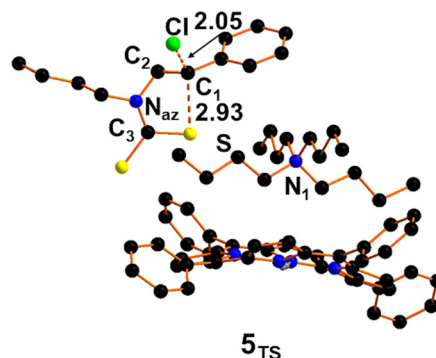

Fig. 3 Optimised structure of transition state **5$_{TS}$**.

formation of the N_{az}–C_3 bonding with a distance of 2.26 Å together with a corresponding 31° bent of the firstly linear CS_2. After the Transition State, the complete formation of the N_{az}–C_3 bonding in **4** occurred with a large free energy gain of -25.5 kcal mol^{-1}.

Due to the loss of symmetry, the original neutral CS_2 moiety acquires a net charge of *ca.* -1 e$^-$ on the sulphur atoms, which are enough electron-rich to perform a nucleophilic attack at the C_1 atom of the opened aziridine of **3^{Bu}**. This process occurs by-passing a very small free energy barrier of $+3.7$ kcal mol^{-1} that allows achieving the Transition State **5$_{TS}$** (Fig. 3).

Even if the sulphur is particularly distant from C_1 (the S–C_1 distance is 2.93 Å) in the transition state **5$_{TS}$**, it can exert its nucleophilic action toward the C_1 centre in a S_N2 fashion forming an S–C_1–Cl angle of 156°. The approach of the sulphur atom to the C_1 centre allows a weakening of the corresponding C_1–Cl distance by *ca.* 0.2 Å, which elongates up to 2.05 Å. The Transition State nature of **5$_{TS}$** was confirmed by the detection of a single imaginary frequency at -60.3 cm^{-1} associated with the approach of the sulphur atom to C_1 and the cleavage of the C_1–Cl bond. It is noteworthy that the resulting energy barrier required for the formation of **5$_{TS}$** is *quasi* three times smaller than that calculated in the same process involving CO_2 (3.7 *vs.* 9.4 kcal mol^{-1}). After the accomplishment of **5$_{TS}$**, the system evolves forming the final thiazolidine-2-thione **5** with a free energy gain of -39.2 kcal mol^{-1} and releasing the chloride anion and the adduct **1**, which can restart the catalytic cycle.

The overall free energy gain for the cycloaddition reaction of CS_2 to *N*-butyl-2-phenylaziridine forming **5** is of -14.5 kcal mol^{-1}. A complete schematic representation of the overall mechanism with all the main intermediates and Transition States that are involved in the CS_2 cycloaddition to *N*-butyl-2-phenylaziridine is shown in Fig. 4.

CS_2 cycloaddition to *N*-aryl aziridine. Even if the CS_2 cyclo-addition to *N*-aryl aziridines was less experimentally explored than the same reaction involving *N*-alkyl or *N*-benzyl deriva-tives, this process deserves to be theoretically investigated in view of potential biological and pharmaceutical properties of analogous molecules obtained from *N*-aryl aziridines and CO_2

(*e.g.* Linezolid,[31] Tedizolid[32] and Toloxatone[33] are oxazolidi-nones already used in therapy).

Analogously to what was discussed above for the reaction involving *N*-butyl-2-phenylaziridine, the starting point of the computational analysis is the analysis of the structure of intermediate **3^{Ar}**.

As a general consideration for all the steps precedent to the formation of **3^{Ar}**, the encountered free energy barrier associated with the achievement of **3^{Ar}$_{TS}$** (the rate determining step of the reaction) is lower than that found for the formation of **3^{Bu}$_{TS}$** due to the presence of CF_3 substituents, which render the aziridine ring very electron-poor, as also confirmed by the calculated electrophi-licity index. The EWGs placed onto the aromatic substituent of the aziridine nitrogen atom (called N_{az}) are also responsible for a limited availability of its electron pair in the activation of inert substrates such as CO_2 and CS_2. The nucleophilicity index for the species **3^{Ar}** was evaluated, revealing a nucleophilicity Nu index of 1.2 eV and a local nucleophilic character for the nitrogen Nu_{Naz} of 0.43 eV smaller with respect to that obtained by modelling *N*-butyl species. This assumption is confirmed by the higher encountered free energy barrier for the very limited free energy gain associated with the formation of the corresponding **3^{Ar}**/CO_2 (1.7 kcal mol^{-1}) and **3^{Ar}**/CS_2 (-1.0 kcal mol^{-1}) adducts.

The optimised structure of the adduct **6** between **3^{Ar}** and CS_2 (Fig. 5) shows a bent alignment of the CS_2 moiety and a new N_{az}–C_3 bond of 1.46 Å, which results in an increase in the length by 0.07 Å with respect to that calculated by modelling *N*-butyl-2-phenylaziridine, suggesting again the weaker donor power of the lone pair placed on the N_{az} centre.

As occurred for the reaction involving *N*-butyl-2-phenylaziridine, also in this case an IR peak related to the symmetric stretching of the CS_2 appears at 582 cm^{-1}, 30 cm^{-1} blue shifted with respect to that observed for adduct **4**, to confirm the less donor power of N_{az} when linked to aryl CF_3-substituted groups. As stated for **4**, also for the formation of the intermediate **6** we isolated a Transition State, namely **6$_{TS}$**, (Fig. 5) with a free energy barrier of $+12.4$ kcal mol^{-1}. After that, the system gains -13.4 kcal mol^{-1} for the complete formation of the C_3–N_{az} bonding in **6**. In **6$_{TS}$**, the CS_2 approaching N_{az} becomes bent by *ca.* 28° already at a long distance of 2.43 Å. The Transition State nature was confirmed by the detachment of a single imaginary frequency at -181.7 cm^{-1}.

In **6** the electron donation from the nitrogen centre confers a sufficient nucleophilicity to sulphur atoms for attacking C_1 in a S_N2 mechanism. The so-formed Transition State **7$_{TS}$** (Fig. 6) shows a *quasi*-linear S–C_1–Cl bond with an angle of 166°.
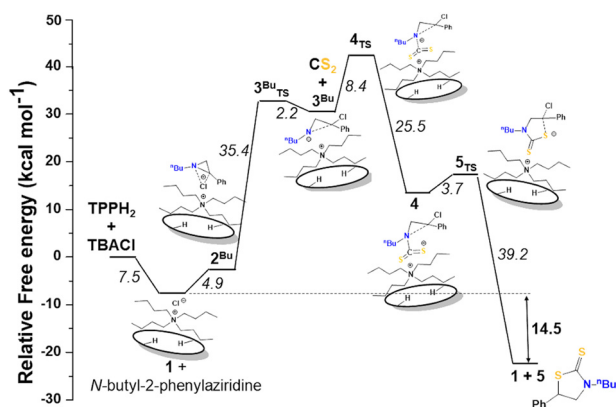

Fig. 4 Free energy profile (kcal mol^{-1}) associated with the synthesis of **5** catalysed by the TPPH$_2$/TBACl system.
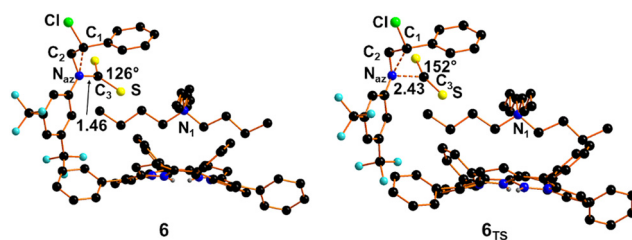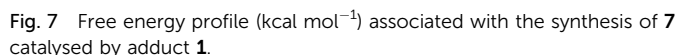

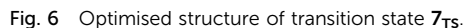**Fig. 5** Optimised structure of the adduct **6** and the transition state **6$_{TS}$**.

Fig. 6 Optimised structure of transition state 7_{TS}.

Fig. 7 Free energy profile (kcal mol^{-1}) associated with the synthesis of **7** catalysed by adduct **1**.

The free energy barrier required for the achievement of 7_{TS} is estimated to be +7.8 kcal mol^{-1} and it is associated with an imaginary IR frequency at −40 cm^{-1}. At this point, *N*-aryl-thiazolidine-2-thione **7** is formed and the adduct **1** regenerated with a free energy gain of −30.9 kcal mol^{-1}.
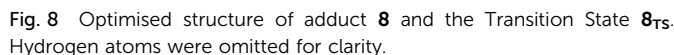
A detailed free energy pathway for the synthesis of *N*-aryl-thiazolidine-2-thione **7** catalysed by the TPPH$_2$/TBACl system is depicted in Fig. 7. The estimated free energy associated with the formation of **7**, starting from CS$_2$ and the model *N*-aryl-2-phenylaziridine, is −7.8 kcal mol^{-1}.

Bifunctional TPPH$_4$Cl$_2$ catalyst for the CS$_2$ cycloaddition to *N*-alkyl aziridines

In view of the already reported DFT studies describing the CO$_2$ activation by the bifunctional TPPH$_4$Cl$_2$ catalysts,[26] the CS$_2$ cycloaddition to *N*-alkyl aziridines in the presence of the same catalyst was theoretically investigated.
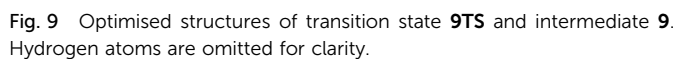
The chlorohydrate TPPH$_4$Cl$_2$ porphyrin, whose formation by the protonation of TPPH$_2$ in THF has been estimated to be exergonic of −31.5 kcal mol^{-1}, can interact with *N*-butyl-2-phenylaziridine and CS$_2$ forming adduct **8** (Fig. 8) with a free energy cost of +29.6 kcal mol^{-1}. This high energy barrier is mainly due to entropic factors since the enthalpy cost is only +4.3 kcal mol^{-1}.

As shown in Fig. 8, the structure of adduct **8** shows a non-linear CS$_2$ molecule with a S–C–S angle of 131° and a new N$_{az}$–C$_3$ bond of 1.54 Å is formed. The transition state 8_{TS} for the obtainment of intermediate **8** was also isolated with a free energy

Fig. 8 Optimised structure of adduct **8** and the Transition State 8_{TS}. Hydrogen atoms were omitted for clarity.

barrier of 33.7 kcal mol^{-1} after which the system gains −4.3 kcal mol^{-1}. Even if the energy barrier was particularly high, the formation of **8** could reasonably occur by employing the same experimental conditions (temperatures higher than 80 °C) required for CO$_2$ activation.[21–26] The high temperature reasonably allows overcoming the high estimated energy barrier.

As shown in Fig. 8, in the Transition State 8_{TS} the CS$_2$ moiety is approaching the aziridine nitrogen at a N$_2\cdots$C$_3$ distance of 2.25 Å. The CS$_2$ in 8_{TS} appears already bent by *ca.* 30° compared to the starting linear arrangement. The Transition State nature of 8_{TS} has been confirmed by the detection of a unique imaginary frequency at −144 cm^{-1} associated with the CS$_2$ approaching as well as the bending of the triatomics. The interaction between the N$_{az}$ centre and the CS$_2$ moiety is also responsible for the electronic depletion of the aziridine ring that makes more favourable the nucleophilic attack of the chloride anion on the more substituted carbon (C$_1$) of the three-membered ring. The less rich electron feature of the aziridine ring after the interaction with CS$_2$ is confirmed by the detection of the transition state **9TS** (Fig. 9) in which the chloride anion can approach the C$_1$ centre overcoming the low free energy barrier of 5.9 kcal mol^{-1}. Comparing the structure of 9_{TS} with a similar Transition State observed in the process involving CO$_2$, the chloride anion seems to be a less efficient nucleophile due to the presence of a Cl–C$_1$ distance shorter by 0.2 Å with respect to that detected in the case of CO$_2$ (1.88 Å). These data suggest a lower electron transfer from the aziridine N$_{az}$ to the CS$_2$ moiety, as also confirmed by the higher free energy barrier required for the formation of 9_{TS} (5.9 *vs.* 1.5 kcal mol^{-1} for CS$_2$ and CO$_2$ cases, respectively). After the obtainment of the Transition State 9_{TS}, the system evolves to the intermediate **9** (Fig. 9) with a free energy gain of −25.1 kcal mol^{-1}. The process is associated with the formation of a new Cl–C$_1$ bond and the complete cleavage of the N$_{az}$–C$_1$

Fig. 9 Optimised structures of transition state **9TS** and intermediate **9**. Hydrogen atoms are omitted for clarity.
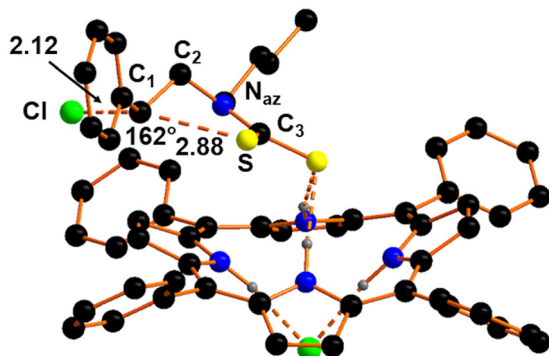
Fig. 10 Optimised structure of transition state **10$_{TS}$**.

linkage. At this point the sulphur atoms of intermediate **9** are nucleophilic enough to attack the C$_1$ atom allowing the ring-closing reaction required for the formation of product **5**.

The ring-closing reaction and the release of the chloride anion occur through the formation of transition state **10$_{TS}$** (Fig. 10) reached by-passing a low free energy barrier of 2.8 kcal mol^{-1}.

In the transition state **10$_{TS}$** the C$_1$ centre achieves a bipyramidal trigonal arrangement with the chloride and one sulphur atom lying quasi co-linear (the S–C$_1$–Cl angle is 162°) at the two apical positions.

The free energy gain from **10$_{TS}$** to achieve the *N*-butyl-thiazolidine-2-thione **5**, together with the restoration of TPPH$_4$Cl$_2$, is of −28.9 kcal mol^{-1}. A detailed free energy reaction pathway for the CS$_2$ cycloaddition to *N*-butyl-2-phenylaziridine catalysed by the bifunctional TPPH$_4$Cl$_2$ molecule is summarised in Fig. 10.

It is interesting to note that despite the use of different catalytic systems (the binary TPPH$_2$/TBACl or the bifunctional TPPH$_4$Cl$_2$ catalyst), the overall free energy gain to provide thiazolidine-2-thione **5** is comparable. In fact, the energy gain to achieve **5** is −14.7 kcal mol^{-1} when TPPH$_4$Cl$_2$ is employed as the catalyst (Fig. 11) and −14.5 kcal mol^{-1} if the binary TPPH$_2$/TBACl system is used (Fig. 4). The energetic similarity between the two catalytic processes is also in agreement with the values previously estimated for the synthesis of *N*-alkyl oxazolidin-2-ones in which the resulting energy gain for the CO$_2$ cycloaddition to the *N*-butyl-2-

phenylaziridine is equal to 4.7 kcal mol^{-1} using either the TPPH$_4$Cl$_2$[26] or the TPPH$_2$/TBACl system.[22]

Experimental

Computational details

All the compounds along the reaction pathway were isolated at the B97D-DFT level of theory[34] within Gaussian 16 package.[35] All the obtained structures were validated as minima or transition states by the vibrational frequencies calculations. The experimental solvent, tetrahydrofuran, has been considered within the CPCM model.[36] The 6-31G basis set, with the addition of the polarization functions (d,p), was adopted. The coordinates of all the optimised structures as well as their main energetic features are reported in the ESI.†

Conclusions

The present manuscript describes a detailed theoretical investigation on the feasibility of the CS$_2$ cycloaddition to *N*-alkyl and *N*-aryl aziridines promoted by metal-free porphyrin-based systems. The performed DFT studies highlighted that either the binary TPPH$_2$/TBACl system or the bifunctional TPPH$_4$Cl$_2$ catalyst could be competent for the synthesis of thiazolidine-2-thiones. The exhaustive study of the possible involved intermediates and Transition States has shown that thiazolidine-2-thiones can be synthesised through reaction mechanisms quite similar to those already suggested in the case of CO$_2$ cycloaddition to aziridines. The TPPH$_2$/TBACl system can promote the synthesis of both *N*-alkyl and *N*-aryl thiazolidine-2-thiones with an overall energy gain of −14.5 kcal mol^{-1} and −7.8 kcal mol^{-1}, respectively. The acquired data are in accordance with the lower reactivity of *N*-aryl aziridines with respect to the *N*-alkyl ones.

In view of the possibility of replacing the TPPH$_2$/TBACl binary system with a cheaper system, eco-compatible bifunctional TPPH$_4$Cl$_2$ species, the CS$_2$ cycloaddition to *N*-alkyl aziridines in the presence of this catalyst was also theoretically investigated. The obtained data revealed the formation of an active intermediate in which the protonated porphyrin can simultaneously activate CS$_2$ and *N*-alkyl aziridine. The overall energy gain of the process was estimated to be 14.7 kcal mol^{-1}. This value is comparable to that calculated for the reaction catalysed by the TPPH$_2$/TBACl binary system to confirm the possibility of employing either the binary porphyrin-based system or the bifunctional porphyrin-based catalyst for the synthesis of *N*-alkyl thiazolidine-2-thiones.

In all the investigated cases, the CS$_2$ cycloaddition to the aziridine rings yielded better results than the same process involving carbon dioxide suggesting the synthetic applicability of the procedure. Future efforts need to be focused on testing the TPPH$_2$/TBACl system and the TPPH$_4$Cl$_2$ catalyst as promoters for the synthesis of thiazolidine-2-thiones.

Conflicts of interest
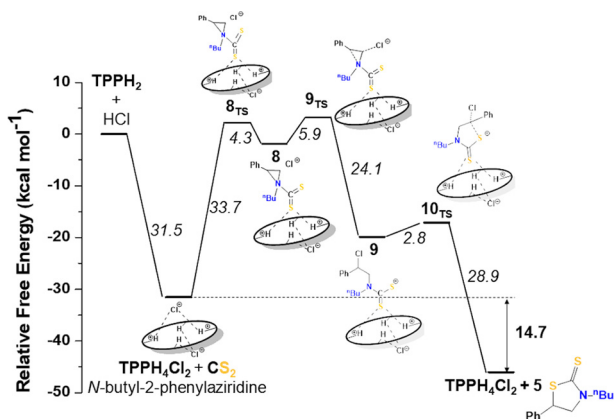
There are no conflicts to declare.

Fig. 11 Free energy profile (in kcal mol^{-1}) associated with the synthesis of **5**, catalysed by the bifunctional TPPH$_4$Cl$_2$.

Acknowledgements

References

1 P. K. Sharma, A. Amin and M. Kumar, *Open Med. Chem. J.*, 2020, **14**, 49–64.

2 F. Velazquez and H. Olivo, *Curr. Org. Chem.*, 2002, **6**, 303–340.

3 A. Degterev, A. Lugovskoy, M. Cardone, B. Mulley, G. Wagner, T. Mitchison and J. Yuan, *Nat. Cell Biol.*, 2001, **3**, 173–182.

4 M. X. Wang, H. W. Qin, C. Liu, S. M. Lv, J. S. Chen, C. G. Wang, Y. Y. Chen, J. W. Wang, J. Y. Sun and Z. X. Liao, *PLoS One*, 2022, **17**, 2–13.

5 Y. S. Prabhakar, V. R. Solomon, M. K. Gupta and S. B. Katti, *Top. Heterocycl. Chem.*, 2006, **4**, 161–249.

6 N. Chen, W. Jia and J. Xu, *Eur. J. Org. Chem.*, 2009, 5841–5846.

7 R. Morales-Nava, M. Fernández-Zertuche and M. Ordóñez, *Molecules*, 2011, **16**, 8803–8814.

8 A. Ziyaei-Halimehjani, K. Marjani and A. Ashouri, *Tetrahedron Lett.*, 2012, **53**, 3490–3492.

9 A. A. Nechaev, A. A. Peshkov, K. Van Hecke, V. A. Peshkov and E. V. Van der Eycken, *Eur. J. Org. Chem.*, 2017, 1063–1069.

10 S. F. Gan, J. P. Wan, Y. J. Pan and C. R. Sun, *Synlett*, 2010, 973–975.

11 A. M. Jacobine and G. H. Posner, *J. Org. Chem.*, 2011, **76**, 8121–8125.

12 S. Gabillet, D. Lecerclé, O. Loreau, M. Carboni, S. Dézard, J. M. Gomis and F. Taran, *Org. Lett.*, 2007, **9**, 3925–3927.

13 A. W. Demartino, D. F. Zigler, J. M. Fukuto and P. C. Ford, *Chem. Soc. Rev.*, 2017, **46**, 21–39.

14 X. F. Jiang, H. Huang, Y. F. Chai, T. L. Lohr, S. Y. Yu, W. Lai, Y. J. Pan, M. Delferro and T. J. Marks, *Nat. Chem.*, 2017, **9**, 188–193.

15 A. Sudo, Y. Morioka, E. Koizumi, F. Sanda and T. Endo, *Tetrahedron Lett.*, 2003, **44**, 7889–7891.

16 T. Able, *J. Org. Chem.*, 2008, 9137–9139.

17 M. Sengoden, M. Vijay, E. Balakumar and T. Punniyamurthy, *RSC Adv.*, 2014, **4**, 54149–54157.

18 A. Khalaj and M. Khalaj, *J. Chem. Res.*, 2016, **40**, 445–448.

19 Y. Xie, C. Lu, B. Zhao, Q. Wang and Y. Yao, *J. Org. Chem.*, 2019, 1951–1958.

20 Y. Shi, B. Tang, X.-L. Jiang, Y.-E. Jiao, H. Xu and B. Zhao, *J. Mater. Chem. A*, 2022, **10**, 4889–4894.

21 D. Carminati, E. Gallo, C. Damiano, A. Caselli and D. Intrieri, *Eur. J. Inorg. Chem.*, 2018, 5258–5262.

22 C. Damiano, P. Sonzini, G. Manca and E. Gallo, *Eur. J. Org. Chem.*, 2021, 2807–2814.

23 P. Sonzini, C. Damiano, D. Intrieri, G. Manca and E. Gallo, *Adv. Synth. Catal.*, 2020, **362**, 2961–2969.

24 C. Damiano, P. Sonzini, M. Cavalleri, G. Manca and E. Gallo, *Inorg. Chim. Acta*, 2022, **540**, 121065.

25 P. Sonzini, N. Berthet, C. Damiano, V. Dufaud and E. Gallo, *J. Catal.*, 2022, **414**, 143–154.

26 A. M. Cavalleri, C. Damiano, G. Manca and E. Gallo, *Chem. – Eur. J.*, 2023, **29**, e202202729.

27 P. K. Chattaraj, S. Duley and L. R. Domingo, *Org. Biomol. Chem.*, 2012, **10**, 2855–2861.

28 L. R. Domingo, M. J. Aurell, P. Pérez and J. A. Saez, *RSC Adv.*, 2012, **2**, 1334–1342.

29 L. R. Domingo, M. Rios-Gutierrez and P. Pérez, *Molecules*, 2016, **21**, 748–760.

30 L. R. Domingo, P. Perez and J. S. Saez, *RSC Adv.*, 2013, **3**, 1486–1494.

31 A. Z. Bialvaei, M. Rahbar, M. Yousefi, M. Asgharzadeh and H. S. Kafil, *J. Antimicrob. Chemother.*, 2017, **72**, 354–364.

32 D. McBride, T. Krekel, K. Hsueh and M. J. Durkin, *Expert Opin. Drug Metab. Toxicol.*, 2017, **13**, 331–337.

33 F. Moureau, J. Wouters, D. Vercauteren, S. Collin, G. Evrard, F. Durant, F. Ducrey, J. Koenig and F. Jarreau, *Eur. J. Med. Chem.*, 1992, **27**, 939–948.

34 S. Grimme, *J. Chem. Phys.*, 2006, **124**, 034108.

35 M. J. Frisch, G. W. Trucks, H. B. Schlegel, G. E. Scuseria, M. A. Robb, J. R. Cheeseman, G. Scalmani, V. Barone, G. A. Petersson, H. Nakatsuji, X. Li, M. Caricato, A. V. Marenich, J. Bloino, B. G. Janesko, R. Gomperts, B. Mennucci, H. P. Hratchian, J. V. Ortiz, A. F. Izmaylov, J. L. Sonnenberg, D. Williams-Young, F. Ding, F. Lipparini, F. Egidi, J. Goings, B. Peng, A. Petrone, T. Henderson, D. Ranasinghe, V. G. Zakrzewski, J. Gao, N. Rega, G. Zheng, W. Liang, M. Hada, M. Ehara, K. Toyota, R. Fukuda, J. Hasegawa, M. Ishida, T. Nakajima, Y. Honda, O. Kitao, H. Nakai, T. Vreven, K. Throssell, J. A. Montgomery Jr., J. E. Peralta, F. Ogliaro, M. J. Bearpark, J. J. Heyd, E. N. Brothers, K. N. Kudin, V. N. Staroverov, T. A. Keith, R. Kobayashi, J. Normand, K. Raghavachari, A. P. Rendell, J. C. Burant, S. S. Iyengar, J. Tomasi, M. Cossi, J. M. Millam, M. Klene, C. Adamo, R. Cammi, J. W. Ochterski, R. L. Martin, K. Morokuma, O. Farkas, J. B. Foresman and D. J. Fox, *Gaussian 16*, Gaussian, Inc., Wallingford CT, 2016, 1.

36 V. Barone and M. Cossi, *J. Phys. Chem. A*, 1998, **102**, 1995–2001.